OPEN ACCESS
Saudi Journal of Civil Engineering
Abbreviated Key Title: Saudi J Civ Eng
ISSN 2523-2657 (Print) |ISSN 2523-2231 (Online)
Scholars Middle East Publishers, Dubai, United Arab Emirates
Journal homepage: https://saudijournals.com/journal/sjce/home

Original Research Article

Assessing the Impact of Extensive Severe Cyclonic Storm Fani on the Coastal Communities of Bangladesh: A Case Study

Mohammad Wahiduzzaman[1*], Gour Chandra Paul[2]

[1]Mathematics Discipline, Khulna University, Khulna 9208, Bangladesh
[2]Department of Mathematics, University of Rajshahi, Rajshahi 6205, Bangladesh

DOI: 10.36348/sjce.2023.v07i02.002 | **Received:** 11.02.2023 | **Accepted:** 18.03.2023 | **Published:** 26.03.2023

***Corresponding author:** Mohammad Wahiduzzaman
Mathematics Discipline, Khulna University, Khulna 9208, Bangladesh

Abstract

This research article presents a numerical simulation of the extensive severe cyclonic storm Fani and its impact along the coast of Bangladesh, which made landfall in the coastal region of Odisha, India, on May 3, 2019. A semi-implicit finite difference method in Cartesian coordinates was employed in this study to solve vertically integrated shallow water equations. The approach allowed for effective forecasting of the storm Fani's impact on the region of choice. Our considered physical domain is discretized with high-resolution gird to cover all the big and small offshore islands. The model predicted water levels for a total of sixteen coastal stations of the Bay of Bengal along the coast of Bangladesh (from 2 May to 03 May 2019, at 3-h interval). Simulated water levels are found closely co-related to the reported data. The simulation results demonstrate that the semi-implicit finite difference method is an effective tool for simulating the storm surge and flooding caused by any severe cyclonic storm. The study also shows that the storm surge and flooding caused by Fani were significant, with a maximum surge height of over 5 meters in some areas. The simulated results provide insights into the spatial and temporal evolution of the storm surge and flooding, which can be useful for designing and implementing appropriate disaster management strategies in the affected regions. Overall, this research article contributes to the scientific understanding of the behavior of severe cyclonic storms and the associated storm surge and flooding, and provides a valuable tool for policymakers and stakeholders to develop and implement effective disaster management strategies in cyclone vulnerable coastal regions.

Keywords: Tropical cyclones, Fani, BOB, ESCS.

1. INTRODUCTION

The Bay of Bengal (BoB) experiences a high frequency of cyclones, particularly on its northeastern side, as reported by Newman and Mandal (1978). Bangladesh is in this region that is particularly vulnerable to tropical storms. The Bay of Bengal (BoB) experiences frequent tropical cyclone formation during two crucial periods: the pre-monsoon season from March to May and the post-monsoon season from October to December. Roughly 7% of all global tropical cyclones originate in the BoB and the Arabian Sea, with the majority of cyclones occurring in the BoB. This ratio is approximately 4:1, as noted by Dube *et al.*, (1997). Coastal cities are at a high risk of experiencing the impacts of climate change, such as sea-level rise, storm surges, flooding, and changes in land use. According to Temmerman *et al.*, (2013), coastal areas with dense populations are highly prone to sea-level rise. The vulnerability of coasta cities to storm surges and flooding caused by tropical cyclones have been studied by Hallegatte *et al.*, (2011), Aerts *et al.*, (2014), Kron (2013), and Woodruff *et al.*, (2013). The alteration of land use in the changing climatic conditions has also been identified as a significant threat to coastal cities (Lal *et al.*, 2020). Geological phenomena such as tsunamis can also contribute to the destruction of coastal cities, as highlighted by Khan *et al.*, (2019). Cyclones are known to cause extensive damage, including loss of life and property, particularly in the adjacent coastal regions. Factors such as shallow bathymetry, flat coastal terrain, low-lying areas, and rising sea surface temperatures are responsible for the cyclogenesis primarily in the BoB, as noted by Gadgil *et al.*, (1984). The primary causative factors for cyclone formation have been studied by Islam and Peterson (2009) and Webster (2008). The impact of severe tropical cyclone 'Fani' in 2019 was reported as the strongest tropical cyclone in the Indian subcontinent

that year and the 10th most severe cyclone in the last 52 years. The cyclone caused significant loss of life and property in eastern and northern India, Bangladesh, and Bhutan. The contribution of heavy precipitation from tropical cyclones around the world has been studied using satellite-based measurements (Jiang and Zipser 2010). The impact of extensive severe cyclone storm (SCS) Fani on water level elevations due to tide, surge, and non-linear TSI is the focus of this study.

2. Event Description of cyclone Fani

On 25th April at UTC 0000, a low-pressure area (LPA) developed over the east Equatorial Indian Ocean (EIO) and adjacent southeast Bay of Bengal (BoB), giving rise to the Extremely Severe Cyclonic Storm (ESCS) named "FANI". As it moved northward on April 26, 2019, its wind speed increased to 50-60 km $h^{-1}$and it became a deep depression. From April 28 to 29, 2019, the depression transformed into a cyclonic storm and moved towards northwest BoB with wind speed increasing to 120-140 km h^{-1}. On April 30, 2019, the cyclonic storm headed northwest towards the Indian coast. By May 2, 2019, Fani had become an extremely severe cyclonic storm with wind speeds of approximately 180-190 km h^{-1} and made landfall at 16° N, 82° E on the Odisha coast. Fani's intensity decreased slightly on May 3, 2019, (175-185 km h^{-1}) as it moved northeast and affected northern Odisha. After May 3, 2019, Fani weakened into a cyclonic storm (130-140 km h^{-1}) and impacted northern Odisha, southern, and central West Bengal. By May 4, 2019, Fani had reduced in intensity (wind speed of 90-100 km h^{-1}) primarily in the West Bengal and Bangladesh region. On May 5, 2019, Fani reached Assam with a low wind intensity of 50-60 km h^{-1} as a deep depression before dissipating. The Sentinel 1B SAR satellite data monitored the eye of Fani in the BoB on May 3, 2019. According to the trajectory-related study, Fani traveled a long trajectory (2136.39 km; 67.25% of the total trajectory) in the ocean (BoB), which provided it with substantial strength and moisture to travel a long distance over land. Fani with a high-intensity (maximum wind speed up to 180 km h^{-1}) severely impacted a large area in the eastern Indian subcontinent, including Odisha, West Bengal, Bangladesh, and Assam. The detailed path history of Fani 2019 is given in Fig. 4 and Table-2 for better perspective.

2.1. Damages caused by Fani in Bangladesh

At least 17 individuals lost their lives, and over 100 people sustained injuries due to Cyclone Fani. The aftermath of the cyclone affected more than 1.6 million people, with many losing their homes and means of livelihood. The disaster also led to the destruction or damage of over 100,000 houses, leaving numerous individuals homeless. Agricultural crops and livestock were severely impacted, with approximately 57,000 hectares of crops destroyed. Moreover, the cyclone caused disruptions in electricity and communication networks, affecting millions of individuals. Transportation problems arose due to damaged roads and bridges, hindering the relief efforts. Water supply systems were disrupted, leading to a shortage of clean water in various areas. According to the United Nations, the estimated cost of damages caused by Cyclone Fani in Bangladesh was around $359 million USD. The government and international aid organizations provided assistance and relief efforts to those affected by the storm.

2.2. Salient Features of Fani

According to the IMD, the severe cyclonic storm Fani that struck the Indian coast on May 3, 2019, had several noteworthy features that made it a significant event in the history of cyclones in the BoB. One of the most unusual features of Fani was its rapid intensification within 24 hours. Starting as a low-pressure area, it quickly intensified into a very severe cyclonic storm with a maximum sustained wind speed of 175 km h^{-1}, making it one of the fastest-intensifying cyclones in recent times. Additionally, it was the most intense cyclone to cross Odisha coast after cyclone Phailin in 2013, with a maximum sustained wind speed of 215 km h^{-1}. Fani was also considered as one of the longest tropical cyclones in the history of the North Indian Ocean, lasting approximately 8 days and 9 hours (Singh *et al.*, 2021). It developed near the equator, a rare occurrence over the north Indian Ocean, and had one of the longest tracks of 3030 km as aforementioned. Furthermore, it had a clockwise recurving track and was mainly steered by an anticyclonic circulation in middle and upper tropospheric levels to the northeast of the system center. As in IMD, the cyclone's rapid intensification during 29th afternoon to 30th April evening over west-central BoB was mainly due to higher ocean heat content, with an increase in maximum sustained wind speed from 45 knots at 0900 UTC of 29th to 95 knots at 1500 UTC of 30th April.

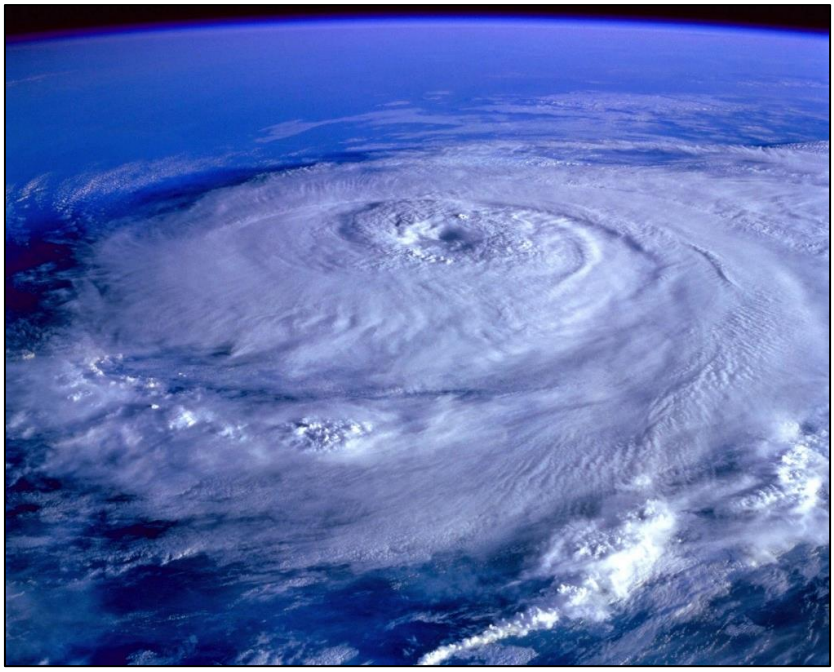

Fig. 1: Tropical storm Fani (Source: NASA Earth Observatory / Joshua Stevens)

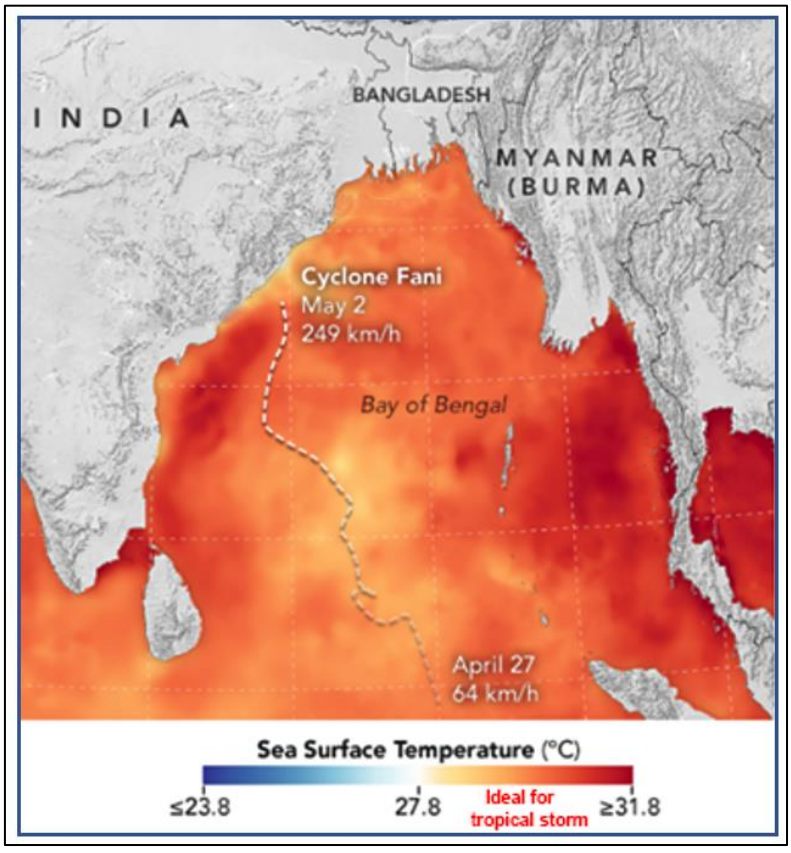

***Fig. 2: Sea surface temperature and storm track information of cyclone Fani (Source:* NASA Earth Observatory / Joshua Stevens)**

3. Impacted geographical areas

The cyclone Fani had a widespread impact on Bangladesh, affecting a total of 28 districts in three different ways. The southern coastal districts experienced tidal inundation with storm winds, while the mid and mid-western districts faced high winds. The entire country also experienced heavy rainfall. The average tidal sea water height during the cyclone was 1-2 feet, which was similar to what the coastal low-lying areas typically experience due to high lunar tides.

Table 1: Damages at a glance

Damages of Cyclone Fani at a glance			
Number of Death	14	Damaged Crop (Fully) in acre	1830
Number of Injured	832	Damaged Crop (Partially) in acre	1,53,832
Dead Livestock	175	Damaged Embankment (KM)	21.95
Damaged HH (fully)	2363	Number of Inundated Villages	59
Damaged HH (Partially)	18670	Number of District Exposed	28
Source: NDRCC preliminary Report (as of 5th May, 2019)			

4. Model Description, Data, and Methodology

The study investigates WLs caused by a tropical storm based on the following vertically integrated shallow water equations (SWEs) (Ali and Paul, 2022):

$$\frac{\partial \zeta}{\partial t} + \frac{\partial \tilde{u}}{\partial x} + \frac{\partial \tilde{v}}{\partial y} = 0, \quad (1)$$

$$\frac{\partial \tilde{u}}{\partial t} + \frac{\partial}{\partial x}(u\tilde{u}) + \frac{\partial}{\partial y}(v\tilde{u}) - f\tilde{v} = -g(\zeta + h)\frac{\partial \zeta}{\partial x} - \frac{1}{\rho}\frac{\partial p_a}{\partial x} + \frac{T_x}{\rho} - c_f \tilde{u}\frac{(u^2+v^2)^{\frac{1}{2}}}{(\zeta+h)}, \quad (2)$$

$$\frac{\partial \tilde{v}}{\partial t} + \frac{\partial}{\partial x}(u\tilde{v}) + \frac{\partial}{\partial y}(v\tilde{v}) + f\tilde{u} = -g(\zeta + h)\frac{\partial \zeta}{\partial y} - \frac{1}{\rho}\frac{\partial p_a}{\partial y} + \frac{T_y}{\rho} - c_f \tilde{v}\frac{(u^2+v^2)^{\frac{1}{2}}}{(\zeta+h)}. \quad (3)$$

In Eqs. (1)-(3), u and v represent, respectively, the depth-averaged velocity components in the directions of x and y axes; t stands for time; ρ is the sea-water density, which is assumed to be incompressible and homogeneous; $f = 2\Omega\, sin\phi$ is the Coriolis parameter, where Ω and ϕ signify the angular speed of rotation of the earth and the latitude of the place of interest, respectively; g represents the acceleration due to gravity, $(\tilde{u}, \tilde{v}) = (\zeta + h)(u, v)$, $\zeta + h$: instantaneous depth of whole water column and p_a is the atmospheric pressure on the sea surface. As in Ali and Paul (2022), the surface stresses are parameterized by

$$T_x = \rho_a\, C_D\, u_a({u_a}^2 + {v_a}^2)^{\frac{1}{2}} \text{ and } T_y = \rho_a\, C_D\, v_a({u_a}^2 + {v_a}^2)^{\frac{1}{2}}, \quad (4)$$

where ρ_a represents the density of air; C_D (= 0.0028, a value used by several researchers) is the dimensionless surface drag coefficient; u_a, v_a symbolize the surface wind components along the x and y axes, respectively.

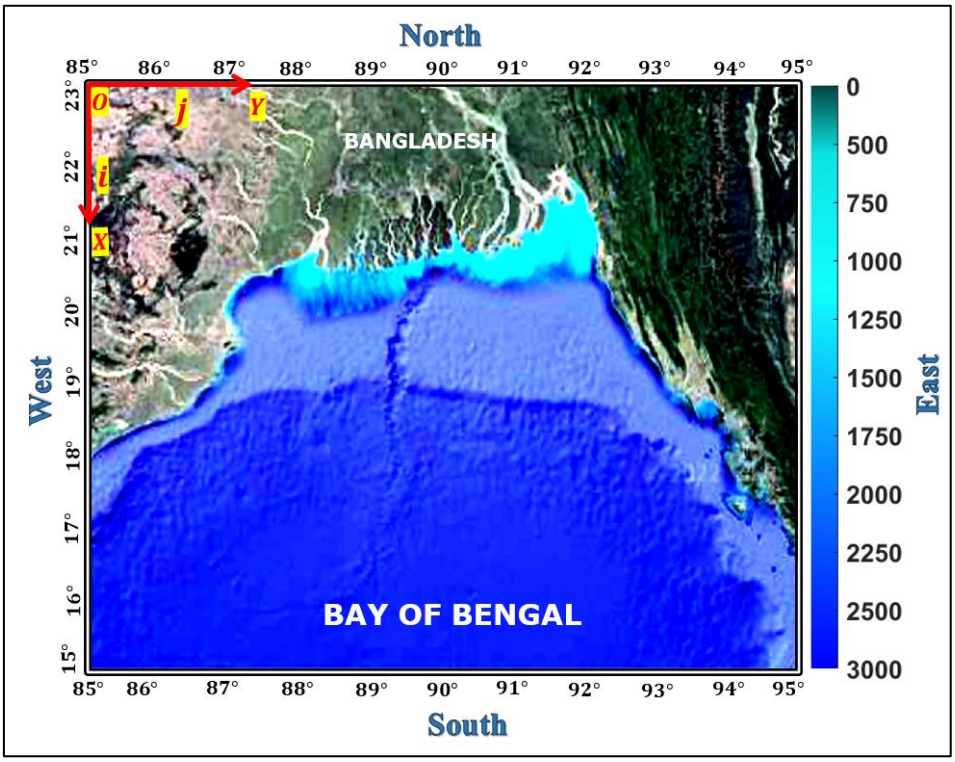

Fig. 3: The domain of the Bay model with Bathymetric information and the Cartesian coordinate system (Source: Google Earth)

For the region of our choice, the most frequently used formula for generating circulatory wind field is due to Jelesnianski (1965), being given by

$$V_a = V_0\sqrt{\left({}^{r_a}/_{R}\right)^3} \text{ for all } r_a \le R \text{ and } V_a = V_0\sqrt{\left({}^{R}/_{r_a}\right)^3}, \text{for } r_a > R, \quad (5)$$

where V_0 is the maximum sustained wind speed at the radial distance R. It is important to mention here that the values of the parameters R and V_0 can be obtained from Bangladesh Meteorological Department (BMD) during any storm along the region of concentration.

The elements of forcing caused by barotropic changes, $\frac{\partial p_a}{\partial x}$ and $\frac{\partial p_a}{\partial y}$ are calculated by (Vickery *et al.*, 2000)

$$p_a(r_a) = p_0 + \Delta p\, exp(-(R/r_a)^{H_0}). \quad (6)$$

Now, it is easy to generate $\frac{\partial p_a}{\partial x}$ and $\frac{\partial p_a}{\partial y}$ from Eq. (6.6) as

$$\frac{\partial p_a}{\partial x} = \frac{x-x_c}{r_a}\,\frac{R\,\Delta p_a\,H_0}{r_a^2}\,exp(-(R/r_a)^{H_0}), \quad (7)$$

$$\frac{\partial p_a}{\partial y} = \frac{y-y_c}{r_a}\,\frac{R\,\Delta p_a\,H_0}{r_a^2}\,exp(-(R/r_a)^{H_0}), \quad (8)$$

where $r_a = \sqrt{(x-x_c)^2 + (y-y_c)^2}$ in which (x_c, y_c) represents the centre of the storm.

In Eqs. (6)-(8), H_0 is Holland's radial pressure profile parameter. It is of interest to note here that H_0 lies between 1 and 2.5 (Holland, 1980), whereas in our present study, H_0 is set to 2.00; ΔP_a is the central pressure deficit and R is aforesaid.

The following RBCs are used along the west, east, and south open boundaries, respectively (see Paul *et al.*, 2016):

West boundary condition: $+\left(\frac{g}{h}\right)^{\frac{1}{2}}\zeta = 0$. (9)

East boundary condition: $-\left(\frac{g}{h}\right)^{\frac{1}{2}}\zeta = 0$. (10)

South boundary condition: $u - \left(\frac{g}{h}\right)^{\frac{1}{2}}\zeta = -2\left(\frac{g}{h}\right)^{\frac{1}{2}}\sum_{i=1}^{4} a_i\, sin\left(\frac{2\pi}{T_i} + \phi_i\right)$. (11)

In Eqs. (9) -(11), a_i is the amplitude of the ith tidal constituent with period T_i and ϕ_i is its phase.

In our model, freshwater discharge from the Meghna River is incorporated along the north-east open boundary segment. At this segment, u_b, the x-component of velocity can be put following Roy (1995) as

$$u_b = u + \frac{Q}{(\zeta+h)\,B}, \quad (12)$$

where Q is the freshwater discharge from Meghna River in m^3s^{-1} and B is the river breadth in m.

5. Numerical Experiments

5.1. Setting up the Strategies

In order to develop an effective warning system, the domain size must be big enough, for a storm to move over it for at least 48 hours before reaching the coast (Rahman *et al.*, 2017). To accurately include the intricate interface of land and sea (see Fig. 3) and to represent the irregularly shaped offshore islands and bathymetry with precision, a higher spatial resolution is required. However, this level of detail necessitates a smaller time step to meet the CFL stability criterion. Therefore, the study implements a high-resolution scheme that can be capable of capturing the coastal complexities depicted in Fig. 3 accurately within the range of 15°-23° N latitude and 85°-95° E longitude in the BoB.

5.2. Model Data Configuration and Model Execution

The numerical experiments are performed with Fani, a SCS. The time variation of the position, central pressure, maximum sustained surface wind (MSSW), and the nature of the storm are tabulated in Table. 2 for a better perspective. Eqs. (1) -(3) and the BCs given by Eqs. (9) -(11) are solved by a conditionally stable semi-implicit FTCS (forward in time and centered in space) FDM on an Arakawa C-grid. The involved parameters have been assumed to have their standard values, such as $= 9.8\ \text{m s}^{-2}$, $\rho = 1025\ \text{kg m}^{-3}$, $\rho_a = 1.226\ \text{kg m}^{-3}$, $\Omega = 0.0174532\ \text{s}^{-1}$, $C_f = 0.0026$. Initially, the values of ζ, u, and v are assumed to be zero to represent a cold start, such a consideration is supported by several studies (see e.g., Zhang *et al.*, 2007). A time step of 10 s is used that ensured the CFL criterion of stability.

5.3. Analysis of Results and Model Validation

For the extremely SCS Fani, the results depending on the tracks (see Tables 2) were computed from 1800 UTC on 26 April to 0200 UTC on 30 April at some stations along the COB. We have chosen 16

stations from the three coastal plains, namely Ganges tidal plain (GTP): Hiron Point, Tiger Point, Patharghata, Kuakata, Rangabali, in Meghna deltaic plain (MDP): Char Madras, Char Jabbar, Char Chenga, Companigonj, Sandwip, and in Chittagong straight plain (CSP): Mirshari, Shitakunda, Chittagong, Bashkhali, Moheshkhali, and Cox's Bazar to display our results for the purpose of analyses.

Table 2: Best track positions and other parameters of the extremely SCS "Fani" over east EIO and adjoining southeast BoB during 26th April – 4th May, 2019

DATE	TIME (UTC)	CENTRE LATITUDE ^{O}N/ LONGITUDE ^{O} E		ESTIMATED MSSW (KT)	ESTIMATED CENTRAL PRESSURE (HPA)	ESTIMATED PRESSURE DROP AT THE CENTRE (HPA)	GRADE
26/04/2019	0300	2.7	89.7	25	998	4	D
	0600	3.0	89.4	25	998	4	D
	1200	3.2	89.2	25	998	4	D
	1800	3.7	88.8	25	998	4	D
27/04/2019	0000	4.5	88.8	30	997	5	DD
	0300	4.9	88.7	30	996	6	DD
	0600	5.2	88.6	35	995	7	CS
	0900	5.4	88.5	40	994	8	CS
	1200	5.9	88.5	45	992	10	CS
	1500	6.3	88.5	45	992	10	CS
	1800	6.6	88.2	45	992	10	CS
	2100	6.9	87.9	45	992	10	CS
28/04/2019	0000	7.3	87.9	45	992	10	CS
	0300	7.3	87.9	45	992	10	CS
	0600	7.4	87.8	45	992	10	CS
	0900	7.7	87.5	45	992	10	CS
	1200	8.2	87.0	45	992	10	CS
	1500	8.3	86.9	45	992	10	CS
	1800	8.4	86.9	45	992	10	CS
	2100	8.5	86.9	45	992	10	CS
29/04/2019	0000	8.6	86.9	45	992	10	CS
	0300	8.7	86.9	45	992	10	CS
	0600	9.2	86.9	45	992	10	CS
	0900	9.7	86.8	45	992	10	CS
	1200	10.1	86.7	55	986	16	SCS
	1500	10.4	86.7	55	986	16	SCS
	1 800	10.8	86.6	55	986	16	SCS
	21 00	11 .1	86.5	60	986	16	SCS
30/04/2019	0000	11.7	86.5	65	980	22	VSCS
	0300	12.3	86.2	75	974	28	VSCS
	0600	12.6	85.7	80	970	32	VSCS
	0900	13.0	85.3	85	966	36	VSCS
	1200	13.3	84.7	90	962	40	ESCS
	1500	13.4	84.5	95	957	45	ESCS
	1800	13.5	84.4	95	957	45	ESCS
	2100	13.6	84.2	95	957	45	ESCS
01/05/2019	0000	13.9	84.0	95	957	45	ESCS
	0300	14.1	83.9	95	957	45	ESCS
	0600	14.2	83.9	95	957	45	ESCS
	0900	14.5	84.1	95	955	45	ESCS
	1200	14.9	84.1	100	950	50	ESCS
	1500	15.1	84.1	100	950	50	ESCS
	1800	15.2	84.1	100	950	50	ESCS
	2100	15.5	84.2	100	950	50	ESCS
	0000	15.9	84.5	105	945	55	ESCS
	0300	16.2	84.6	105	945	55	ESCS
	0600	16.7	84.8	110	940	60	ESCS

02/05/2019	0900	17.1	84.8	115	932	66	ESCS
	1200	17.5	84.8	115	932	66	ESCS
	1500	17.8	84.9	115	934	66	ESCS
	1800	18.2	85.0	115	934	66	ESCS
	2100	18.6	85.2	115	934	66	ESCS
03/05/2019	0000	19.1	85.5	105	945	55	ESCS
	0300	19.6	85.7	100	950	50	ESCS
	0600	20.2	85.9	85	952	46	VSCS
	0900	20.5	86.0	75	970	28	VSCS
	1200	21.1	86.5	70	976	22	VSCS
	1500	21.5	86.7	60	980	18	SCS
	1800	21.9	87.1	55	986	16	SCS
	2100	22.5	87.9	50	990	12	SCS
04/05/2019	0000	23.1	88.2	40	994	8	CS
	0300	23.6	88.8	30	996	6	DD
	0600	24.3	89.3	25	998	5	D
	1200	25.2	90.7	20	1000	4	D
	1800	**Weakened into well marked low-pressure area over central Assam & neighborhood**					

The cyclone that struck on April 26, 2019 and dissipated on May 5, 2019 (becoming a remnant low after May 4) boasted some of the most extreme weather conditions on record. Its 3-minute sustained winds reached 215 km h^{-1} (130 mp h^{-1}), while its 1-minute sustained wind hit an astonishing 280 km h^{-1} (175 mp h^{-1}). The maximum sustained wind radius spanned 50 km, and the storm's lowest pressure was measured at 932 hPa (mbar). The cyclone also caused significant damage and loss of life, with 89 total fatalities and an estimated $8.1 billion (2019 USD) in damages, making it the third costliest cyclone ever recorded in the Indian Ocean.

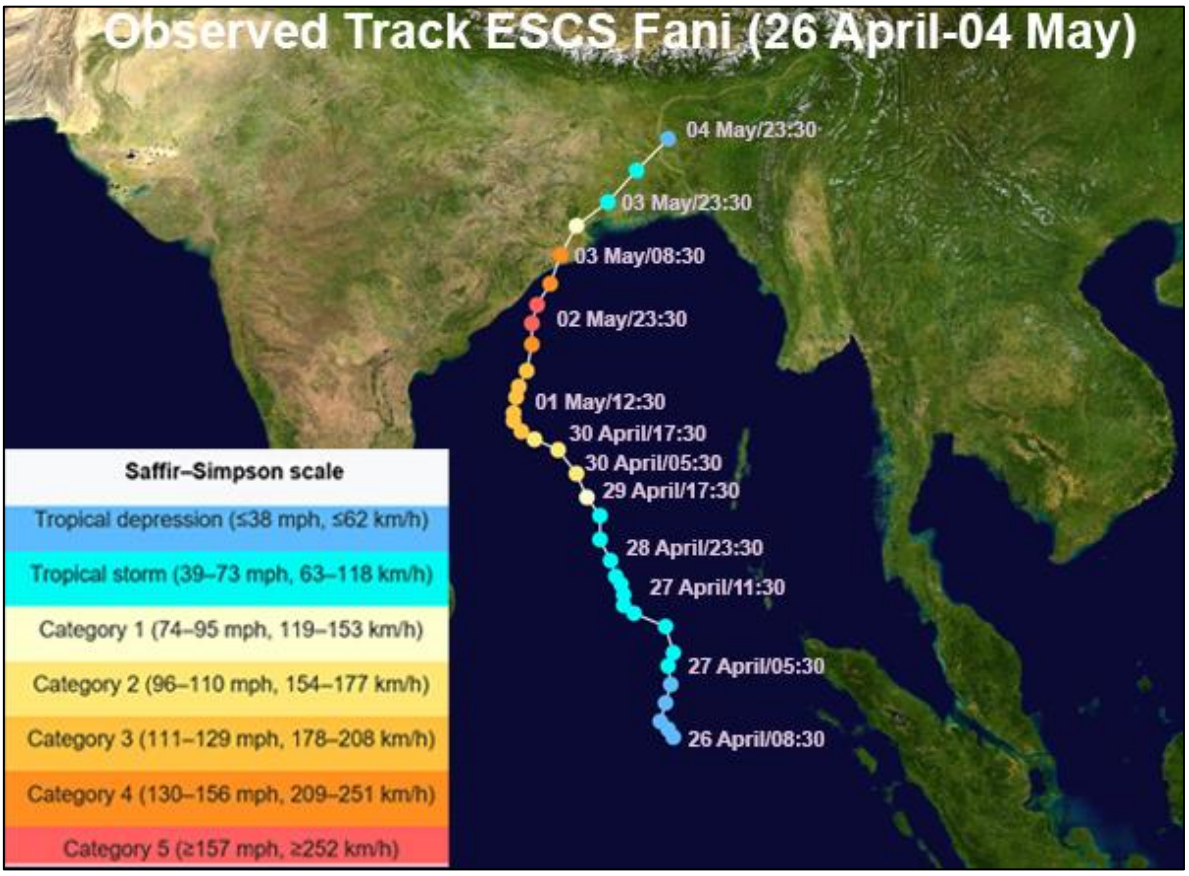

Fig. 4: Life period of cyclone Fani form 26 April-04 May, 2019. (Source: Wikipedia)

6. RESULTS AND DISCUSSION

Fani underwent rapid intensification, developing into an extremely SCS and reaching its peak intensity on May 2nd, with 1-minute sustained wind equivalent to a Category 5 major hurricane. The following day, on May 3rd, the storm made landfall in the East Indian state of Odisha, with sustained maximum wind speeds of 185-195 km h^{-1} and gusts up to 205 km h^{-1} on land. The IMD reported that the storm weakened as it moved north-north-eastwards towards West Bengal and Bangladesh. It was expected to continue in a north-northeasterly direction over the Odisha-West Bengal coastal area and reached Khulna and the adjoining southwestern part of Bangladesh by midnight on May 3, 2019. As of that morning, the Khulna and surrounding coastal areas of Bangladesh had already been experiencing the peripheral effects of the very SCS Fani, with maximum sustained wind speeds within 74 km of the storm center at about 140 km h^{-1}, rising to 160 km h^{-1} in gusts/squalls. As we delve into the results presented in Figures 5, 6, and 7, a remarkable pattern emerges. In Figure 5(a-c), we witness the astounding spectacle of maximum water height due to astronomical tide in the Ganges deltaic plain's Rangabali (1.06 m), Meghna tidal plain's Companigonj (1.21 m), and Chittagong straight plain's Bashkhali (1.34 m). The sheer force of nature is awe-inspiring, reminding us of the remarkable power of the ocean. Turning our attention to Figure 6(a-c), we witness a different manifestation of the sea's might. The maximum water height due to pure surge is nothing short of phenomenal, with Patharghata (1.57 m), Companigonj (3.95 m), and Mirsharai (3.92 m) all experiencing the full brunt of this force in the Ganges deltaic plain, Meghna tidal plain, and Chittagong straight plain, respectively. The magnitude of these numbers is hard to fathom, and yet they serve as a testament to the immense power of the sea. Finally, we witness the dramatic impact of non-linear tide-surge interaction in Figure 7(a-c), with the highest water height observed in Patharghata (2.34 m), Companigonj (4.94 m), and Mirsharai (4.81 m) in the Ganges deltaic plain, Meghna tidal plain, and Chittagong straight plain, respectively. The intricate interplay of tide and surge produces a mesmerizing display of nature's fury, leaving us in awe of the awe-inspiring forces at work in our world.

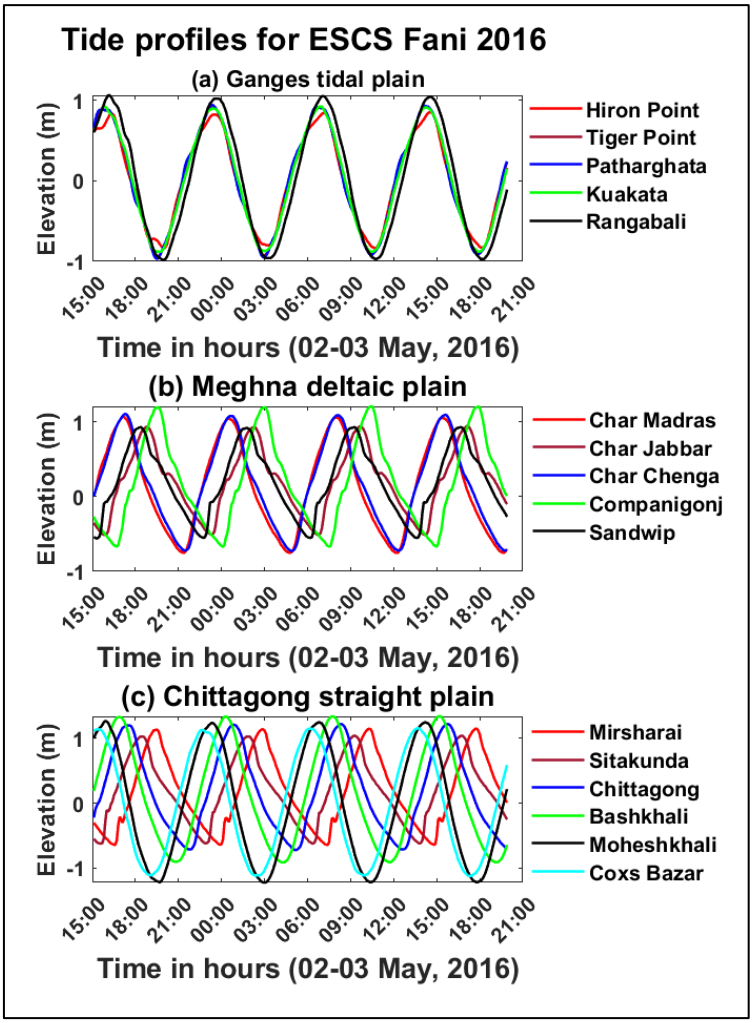

Fig. 5(a-c): Temporal variation of WLs with respect to the MSL due to tide

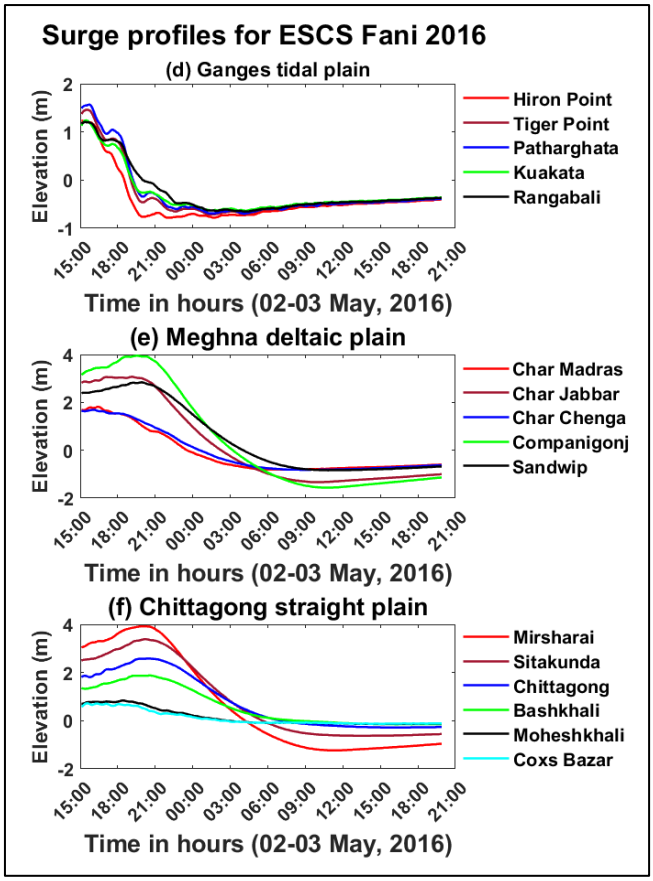

Fig. 6(a-c): Temporal variation of WLs with respect to the MSL due to surge associated with cyclone Fani

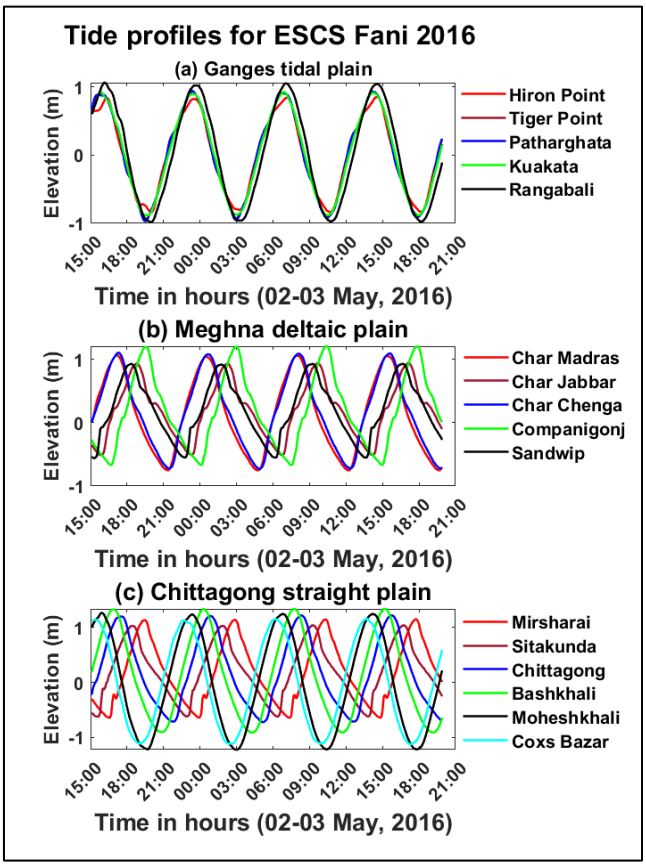

Fig. 7(a-c): Temporal variation of WLs with respect to the MSL due to TSI associated with cyclone Fani

Table 3: Peak WLs due to tide, surge, and TSI

Coastal location	Simulated max. tide level (m)	Simulated max. surge level (m)	Simulated max. TSI level (m)
Hiron point	0.85	1.23	1.94
Tiger point	0.92	1.46	2.22
Patharghata	0.94	1.57	2.34
Kuakata	0.93	1.24	1.99
Rangabali	1.06	1.21	2.12
Char Madras	1.07	1.82	2.53
Char Chenga	1.11	1.69	2.53
Char Jobbar	0.95	3.07	3.81
Companigonj	1.21	3.95	4.94
Sandwip	0.93	2.84	3.51
Mirsharai	1.15	3.92	4.81
Shitakunda	1.04	3.39	3.90
Chittagong	1.22	2.58	3.10
Bashkhali	1.34	1.88	2.68
Moheskhali	1.27	0.84	2.03
Cox's Bazar	1.16	0.72	1.79

7. CONCLUSION

In conclusion, the SCS Fani that struck the Indian coast on May 3, 2019, was a significant event in the history of cyclones in the BoB. This research article aimed to study the storm surge characteristics of Fani using the SWEs and semi-implicit FDM. The model was validated using the reported results. The results of the study showed that Fani caused a high storm surge, with a maximum surge height of over 5 meters in some areas. The storm surge characteristics were influenced by various factors such as the topography of the coastal region, wind speed, and direction. The model was found to be accurate in predicting the water height during the storm, and the validation of the model using reported data adds credibility to the study. The study provides valuable insights into the behavior of cyclones in the BoB and the impact of storm surge on the coastal regions. The results of the study can be used by policymakers and disaster management authorities to develop effective mitigation strategies and evacuation plans. The study also highlights the importance of accurate forecasting of cyclones and the use of advanced technologies and tools in disaster management. In conclusion, this research article contributes to the scientific understanding of storm surge in the BoB and provides a methodology for modeling and predicting the water height during cyclonic storms. The study can serve as a reference for future research in this field and can be used as a basis for the development of early warning systems and disaster management plans.

ACKNOWLEDGMENTS

National Science and Technology (NST) provided partial funding for this research through the Fellowship 2022-2023 under grant number 39.00.0000.012.002.007.22.161, dated 29/12/2022. The first author expresses gratitude for this support.

REFERENCES

- Aerts, J. C. J. H., Lin, N., Botzen, W. J. W., & Emanuel, K. (2014). Evaluating flood resilience strategies for coastal megacities. *Science*, 344(6183), 473–475. https://doi.org/10.1126/science.1248222
- Ali, M. E., & Paul, G. C. (2022). An estimation of water levels associated with a storm along the coast of Bangladesh using a non-central difference method of lines. *Ocean Engineering*, 248, 110776. https://doi.org/10.1016/j.oceaneng.2022.110776
- Dube, S., Rao, A., Sinha, P., Murty, T., & Bahulayan, N. (1997). Storm surge in the Bay of Bengal and Arabian Sea: The problem and its prediction. *Mausam*, 48, 283–304. DOI: https://doi.org/10.54302/mausam.v48i2.4012
- Gadgil, S., Vinayachandran, P. N., & Francis, P. A. (1984). DYNAMICS OF THE BAY OF BENGAL. *Journal of Geophysical Research*, 89(C3), 4549–4558. https://doi.org/10.1029/JC089iC03p04549
- Hallegatte, S., Green, C., Nicholls, R. J., Corfee-Morlot, J. (2011). Future flood losses in major coastal cities. *Nature Climate Change*, 3(9), 802–806. https://doi.org/10.1038/nclimate1979
- Holland, G. J. (1980). An analytic model of the wind and pressure profiles in hurricanes. *Monthly Weather Review*, 108(8), 1212–1218. https://doi.org/10.1175/1520-0493(1980)108<1212:AAMOTW>2.0.CO;2
- India Meteorological Department (2019). Cyclonic storm "Fani" over East-central Bay of Bengal: A report by IMD. Retrieved from http://www.rsmcnewdelhi.imd.gov.in/images/bulletin/cyclone-report/fani.pdf
- Islam, M. S., & Peterson, A. T. (2009). Impacts of sea-level rise on mangrove ecosystems: a region-wide analysis based on model simulations. *Global Ecology and Biogeography*, 18(6), 703–714. https://doi.org/10.1111/j.1466-8238.2009.00461.x

- Jelesnianski, C. P. (1965). A numerical calculation of storm tides induced by a tropical storm impinging on a continental shelf, Mon. *Weather Rev.*, 93, 343-358. https://doi.org/10.1175/1520-0493(1993)093<0343:ANCOS>2.3.CO;2
- Jiang, H., & Zipser, E. J. (2010). Precipitation characteristics of tropical cyclones over the western North Pacific. *Journal of Climate*, 23(6), 1526–1541.https://doi.org/10.1175/2009JCLI3056.1
- Khan, A. A., Kumar, A., & Lal, P. (2019). Spatio-temporal evaluation of long-term earthquake events and its contribution in genesis of tsunami in the Indian ocean. *ISPRS Ann Photogramm Remote Sens Spatial Inf Sci*, IV-5/W2:43–48. https://doi.org/10.5194/isprs -annal s-IV-5-W2-43-2019
- Kron, W. (2013). Coasts: the high-risk areas of the world. *Nat Hazards*, 66, 1363–1382. https://doi.org/10.1007/s11069-012-0215-4
- Lal, P., Prakash, A., Kumar, A., Srivastava P. K., Saikia, P., Pandey, A. C., Srivastava, P., & Khan, M. L. (2020). Evaluating the 2018 extreme flood hazard events in Kerala, India. *Remote Sens Lett*, 11, 436–445. https://doi.org/10.1080/21507 04X.2020.17304 68
- Newman, C. J., & Mandal, G. S. (1978). Statistical prediction of tropical storm motion over the Bay of Bengal and Arabian Sea. *Indian J. Met. Hydrol. Geophys*, 29(2), 487–500. DOI: https://doi.org/10.54302/mausam.v29i3.2921
- Paul, G. C., Ismail, A. I. M., Karim, M. F., Rahman, A., Karim, M. F., & Hoque, A. (2016). Development· of tide-surge interaction model for the coastal region of Bangladesh. *Estuaries and Coasts.*, 39(6), 1582-1599 (2016). doi: 10.1007/s12237-016-0110-4
- Rahman, M. M., Paul, G. C., & Hoque, A. (2017). A shallow water model for computing water level due to tide and surge along the coast of Bangladesh using nested numerical schemes. *Mathematics and Computers in Simulation*, 132, 257–276 (2017). doi: 10.1016/j.matcom.2016.08.007
- Roy, G. D. (1995). Estimation of expected maximum possible water level along the Meghna estuary using a tide and surge interaction model. *Environ. Int.*, 21(5), 671-677. https://doi.org/10.1016/0160-4120(95)00078-Y
- Singh, K. S., Albert, J., Bhaskaran, P. K., & Alam, P. (2021). Assessment of extremely severe cyclonic storms over Bay of Bengal and performance evaluation of ARW model in the prediction of track and intensity. *Theoretical and Applied Climatology*, 143(3), 1181-1194. https://doi.org/10.1007/s00704-020-03510-y
- Temmerman, S., Meire, P., Bouma, T. J., Herman, P. M. J., Ysebaert, T., & De Vriend, H. J. (2013). Ecosystem-based coastal defence in the face of global change. *Nature*, 504, 79–83. https ://doi.org/10.1038/natur e1285 9
- Vickery, P. J., Skerlj, P. F., Steckley, A. C., & Twisdale, L. A. (2000). Hurricane wind field model for use in hurricane simulations. *Journal of Structural Engineering*, 126(10), 1203-1221. https://doi.org/10.1061/(ASCE)0733-9445(2000)126:10(1203)
- Webster, P. J. (2008). Myanmar's deadly daffodil. *Nat Geosci*, 1, 488–490. https://doi.org/10.1038/ngeo257
- Woodruff, J. D., Irish, J. L., & Camargo, S. J. (2013). Coastal flooding by tropical cyclones and sea-level rise. *Nature*, 504, 44–52. https://doi.org/10.1038/nature12855
- Zhang, W. Z., Hong, H. S., & Shang, S. P. (2007). A two-way nested coupled tide-surge model for the Taiwan Strait. *Continental Shelf Research*, 27 (10-11), 1548–1567. doi: 10.1016/j.csr.2007.01.018